The ESO Photometric and Astrometric Analysis Programme for Adaptive Optics

D. CURRIE[a], D. BONACCINI[a]
E. DIOLAITI[b], S. TORDO[a], K. NAESGARDE[a], J. LIWING[a],
O. BENDINELLI[b], G. PARMEGGIANI[c], L. CLOSE[a]

Contact E-mail: dcurrie@eso.org
[a]European Southern Observatory, Garching bei München, Germany
[b]Università di Bologna – Dipartimento di Astronomia, Bologna, Italy
[c]Osservatorio Astronomico di Bologna, Italy

Abstract

The European Southern Observatory is currently developing an array of software analysis packages to perform Photometry and Astrometry (P&A) on both stellar and diffuse objects observed with Adaptive Optics (AO) Systems[1, 2]. As they are completed, the component programmes of ESO-PAPAO will be made available to AO observers using ADONIS on the 3.6-metre telescope at La Silla and later, to those observers using the various AO systems being developed for the 8.2-metre VLT telescopes at Paranal, such as NAOS-CONICA and MACAO-SINFONI.

The performances of the ESO-PAPAO package are being extensively quantified; both to support their use in astrophysical analysis and as a guide for the definition of AO observing programmes. The algorithms are being developed in IDL. A user interface programme (ION) allows immediate access to the ESO-PAPAO by observers not familiar with IDL. We will describe the objectives of the ESO-PAPAO, the calibrated ADONIS data sets that have been collected for distribution to contributors to the ESO-PAPAO programme, and the methods and results of numerical tests of photometric precision in comparing the various different analysis packages. In particular, the STARFINDER[3,4,5] (see this issue, p. 23) programme, developed at the University of Bologna in a collaborative effort with ESO, has been applied to data from ADONIS at La Silla, UHAO at Mauna Kea, and HST. Results from the analysis of this astronomical AO data will be presented, i.e. photometric precision of 0.01 to 0.05 magnitudes and astrometric precision of ~ 0.1 pixel in crowded fields with strong isoplanatic effects. The structure of PAPAO is illustrated in the chart on page 21.

1. Introduction

Over the past decade, the operation of Adaptive Optics Systems, led by the COME-ON > COME-ON+ > ADONIS systems on ESO's 3.6-metre telescope at La Silla, Chile[6, 7], have demonstrated the effectiveness of this technology in the field of high-resolution astronomy.

The optimal extraction of scientifically valid results from AO data can be a difficult operation. The challenges in AO Data Reduction were initially reviewed in 1995–1997 by the AO Data Reduction Working Group, organised by N. Hubin[8]. In 1997–1998, D. Bonaccini and J. Christou installed IDAC, an implementation of myopic deconvolution specially suited to AO data, tested it with real AO data, and made it available to ESO users[9,10]. Today the new IDAC 2.7 is kindly supported by Keith Hege at the University of Arizona, and linked at http://www.ls.eso.org/lasilla/Telescopes/360cat/adonis/html/datared.html . The use of IDAC has been encouraged for AO users with tutorials and performance test procedures, linked at the same Web site. Users are encouraged to provide feedback. However, with the development and imminent deployment of VLT instruments using Adaptive Optics, it has become necessary to provide AO support in photometry, astrometry, and deconvolution for the general observer using these ESO systems. To address this issue, the Photometry and Astrometry Programme for Adaptive Optics (PAPAO) was initiated in September of 1998[1, 2] by D. Currie, D. Bonaccini and F. Rigaut. This recognised the need for specific AO data-reduction algorithms and their software implementations, and for the quantitative comparison of the performance of these packages. The latter will allow the selection of the appropriate package for a specific scientific objective, and the quantification of the precision of the resulting scientific analysis. It is the PAPAO that will be addressed in this paper.

1.1 Classes of Adaptive Optics Data

The primary application of AO to date has been in broad-band imaging, followed by narrow-band imaging (this includes 89% of all referred AO publications[11]). This will be the topic of the current presentation. However, there are a large variety of data types that must be addressed in a similar manner in the near future, that are reviewed elsewhere[1].

2. Motivation and Objectives of PAPAO

The primary objectives of the ESO Photometry and Astrometry Programme for Adaptive Optics (PAPAO) are to provide the tools to define appropriate observational procedures, to reduce the AO data obtained specifically in support of this programme, and to evaluate the precision and accuracy of the results obtained with these new methods of data reduction. These tools will address the general ESO observer, using the ESO AO systems, that is, ADONIS[6, 7], CONICA/NAOS[12], and the AO systems that will be implemented at Paranal in the next few years (e.g. SINFONI). These tools will be publicly available at the Web Sites at ESO and at the PAPAO collaborating institutes as a contribution to AO observers in general.

2.1 Motivation of PAPAO

The observational imaging data obtained from the Adaptive Optics systems have many features that make the extraction of valid scientific results much more challenging than the analysis of images obtained from conventional low-resolution telescope imaging. The Point Spread Function (PSF) has extended wings (similar to the PSF of the Hubble Space telescope prior to the repair mission, due to optical errors in the primary mirror). In addition, the structure of the AO PSF changes over the field of view, and it is not constant in time, neither within a single observation nor from one observation to another (i.e. as one changes filters, maps an area in the sky, or observes a PSF calibration star at a later time).

Starting in October 2001, the CONICA/NAOS system, incorporating a 196-element Shack-Hartmann AO System and a 1–5 micron camera on the VLT (UT3), will start to be used by general astronomers of the ESO community. As an example of the need and motivation for an ESO AO ToolKit, we may look at the history of the publications from the ADONIS system over the past four years of facility operation[11]. In our opinion, up to now, these data-processing problems have reduced the scientific output favouring those with detailed experience, i.e., those who have built the instrument or belong to the institutes that built it.

In order to assure the effective use of CONICA/NAOS and future AO instruments, ESO created the PAPAO programme within the AO Group of the Instrumentation Division to provide a ToolKit of software packages, adapted to the AO systems on the ESO telescopes. In principle, such a package should address a wide range of science aspects, for both photometry and astrometry, and for both stellar and diffuse or nebular objects. It should apply to data obtained with both high and low Strehl ratios and images that are both well-sampled and under-sampled.

2.2 Programme Structure of the PAPAO

The PAPAO programme at ESO consists of three primary components. The first is the collection of algorithms to perform photometry and astrometry which are to be available in a public form, and which are documented for a general observer. The second component, the major current effort, consists of the collection of AO data, both a focused set of observations using ADONIS on the ESO 3.6-metre telescope at La Silla, and the identification and collection of data contributed by astronomers operating on other telescopes with other Adaptive Optics systems. The third component has two parts. The first part is the evaluation of the performance of the candidate software packages for the ESO ToolKit using real telescope data. The second part is the identification of those algorithms, programmes, and elements of programmes, that are particularly effective in photometry and astrometry and which should be developed for inclusion in future versions of the ESO ToolKit.

2.3 Scope and Objectives of PAPAO

The software has a widget interface so that the astronomer does not require a knowledge of any specific programming language. The first element of the ESO ToolKit is STARFINDER[3,4,5], a software programme for stellar photometry being developed in a collaboration between the University of Bologna and ESO. In support of the AO astronomer (but not as part of the PAPAO) are a number of the other software programmes that are available within the ESO System, that is, eclipse (for preprocessing ADONIS and future data from other AO systems in a pipeline manner), IDAC (for myopic deconvolution, and of course the large general packages of MIDAS, IDL and IRAF.

A quantitative evaluation of the performance of the ToolKit packages on real telescope data from AO systems will be provided on the ESO Web Site for PAPAO. The results of this evaluation are a part of the Algorithm Testing portion of the PAPAO programme discussed below.

2.3.1 Relative versus Absolute Photometry

The primary consideration in this discussion will be relative photometry, that is, the relative magnitude of different stars or the relative brightness of components of extended structures within a given frame or image. Of course, this does not address all of the features of a photometric reduction. The procedures connected with the selection, observation and reduction of photometric standard stars is an essential part of the procedure. However, our early tests within the PAPAO indicated that the photometric errors in relative photometry were essentially as large as the published errors in absolute photometry, so we have initially concentrated on the consideration of relative photometry in this programme.

2.3.2 Astronomer interface and programming language

The ToolKit has been developed in the IDL language, from Research Systems, Inc. The TookKit packages operate with a widget user interface. This means that the astronomer does not need to have knowledge of IDL or any other processing language. All of the options and procedures are presented in the form of buttons, with on-line help files available for detailed explanations. The IDL code will be available on the PAPAO Web Site. Concerning the IDL licensing issue, one technically feasible approach for the licensing could be for ESO to operate the ION interface to IDL on the ESO computers. This would allow the remote user to use his own computer and Web Browser to operate these ToolKit programmes on the ESO computer and license. Thus he/she could run the elements of the ToolKit on the ESO computers without a local IDL license, using a browser on his/her PC or workstation at his/her own institution. A demonstration and evaluation of this mode of operation will be conducted in June-July 2000, to evaluate the feasibility and identify any problems. If you are interested in participating in this test to evaluate STARFINDER and the remote operation capabilities of ION, please contact dcurrie@eso.org.

2.4 The Challenge to PAPAO

There are two primary challenges to achieving improvements in photometry and astrometry that parallel the very significant advances in the hardware side of adaptive optics. The first is the complexity and variability of the PSF. In the small patches of Figure 2, we can see the complexity of the wings of PSFs. Although these images have been enhanced to show the fainter stars, the accurate inclusion of the light in these wings is necessary to obtain good photometric accuracy. Comparison of the successive images of the PSF show both the super-speckles that are stable enough that they do not decrease as the square root of N, and the shorter-term effects of the atmosphere. The super-speckles usually remain stable for successive exposures on the target, but can significantly change when going across the sky to a new PSF calibration star. The shorter-term difference can be seen by comparing the differences in the patches that were taken over a few minutes. This is a significant effect in a programme to obtain 1% photometry. In Figure 3, we can see the difference in the PSF at different parts of a single image (the an-isoplanatic effect). Thus a star near the guide star has a near diffraction-limited structure, while an image at the edge of the field of view is highly elongated toward the guide star. Again, this requires extreme care and a good knowledge of the variable PSF to obtain high precision on the photometry of both of those stars. Finally, for the infrared observations addressed in this paper, the proper flat fielding of the images is a major challenge with the current generation of infrared arrays. Even a very well studied system (SOFI at La Silla) achieving 1% flat-fielding is a very large challenge.

Like the situation after the launch of the Hubble Space Telescope, a giant leap in instrumentation has provided a large advance in resolution. However, for WFPC to realise the full measure of science from the improved resolution in the presence of an imperfect PSF required an intense study of the proper role of deconvolution. Neither the spherical aberration of Hubble could, nor the AO data processing challenge can be addressed with quick, short-term solutions.

3. Role and Contents of the ESO ToolKit

In this section, we consider the current and planned elements of the ESO ToolKit. We also discuss the current status of each of these elements.

3.1 STARFINDER – SI – for Spatially Invariant Data

This package of programmes addresses photometric and astrometric measurements of well-sampled stellar sources (i.e. unresolved objects). The interface to the user is a widget-based GUI. This software programme has been developed by Emiliano Diolaiti of the Osservatorio Astronomico di Bologna[3,4,5] in collaboration with ESO. This package of programmes is currently in final testing to assure the proper operation with different versions of IDL, different versions of the astron 19 library and different computer systems. This software package will be distributed on the PAPAO Web Site and from a Web Site at the Osservatorio Astronomico di Bologna. It will also be available in the remote operation test in July-August 2000.

3.2 Astrometric Motion of Nebular Clumps

This programme addresses astrometric measurements of nebular (i.e. extended or diffuse) targets, and was originally developed by Dan Dowling[13, 14, 15] for the analysis of the motion of the clumps of dust and gas in the homunculus of η Carinae. This programme used data from the WFPC prior to the repair mission as well as post-repair data from WFPC2. Thus it has addressed the issues of highly accurate astrometry (at the 5 mas level), both for PSFs with strong and negligible wings (i.e. equivalent to high and low Strehl ratios in AO). The programme has been modified for use with AO in the environment of the ESO ToolKit and tested for astrometric accuracy on real telescope data by Katrin Naesgarde[16] and Johan Liwing[17]. However, it still needs to be packaged for the ToolKit, and the widget interface has not been developed at this time.

3.3 STARFINDER – SV – for Spatially Variant AO Data

This package of programmes addresses AO data in which the an-isoplanatism causes significant changes in the shape of the PSF (and thus in the photometric and astrometric measurements), as a function of the distance to the guide star. This is illustrated in Figure 3. Properly handling anisoplanatism effects in AO data is a much required and original contribution. The proper handling of an-isoplanatic effects in AO data is an essential requirement and this work is a unique contribution. The initial version of this programme has been implemented and tested on real telescope data by Diolaiti et al.[3,4,5]. Discussion of its effectiveness for processing data with very significant an-isoplanatism has been investigated. The code is in the process of being finalised and made into a user programme with a widget interface at the University of Bologna (Italy).

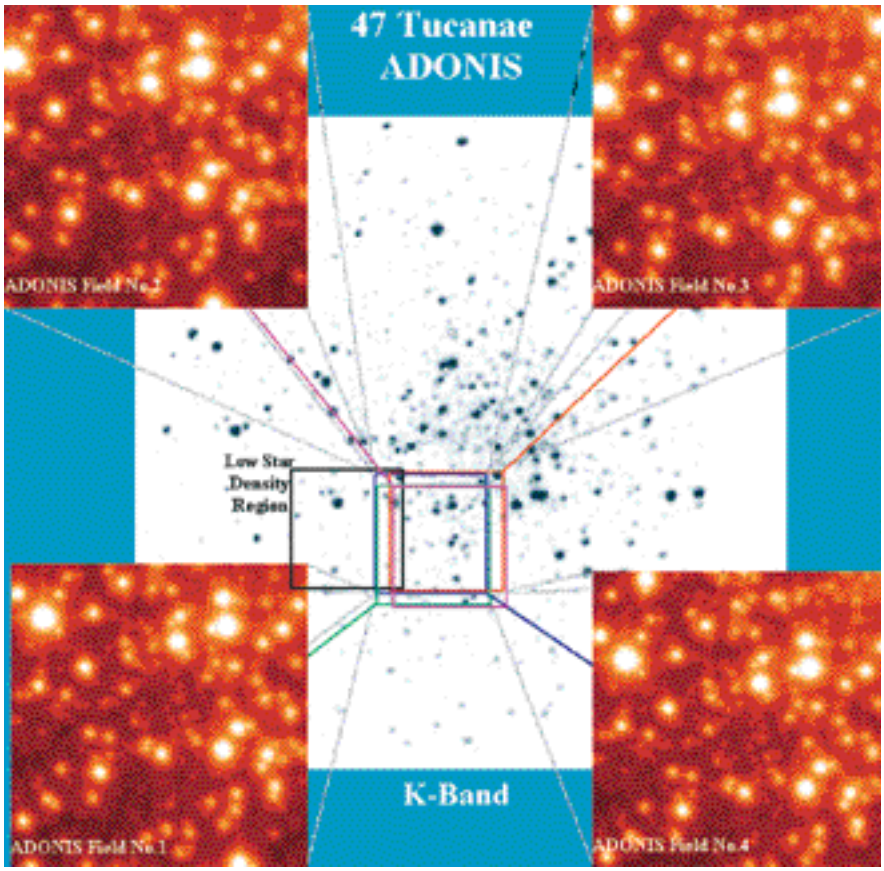

Figure 1 illustrates the type of data that has been collected on ADONIS. This shows the images for the four overlapping pointings obtained by re-pointing the telescope (or more accurately, moving an internal mirror in the ADONIS system). The background is a ground-based K-band image of the centre of the globular cluster 47 TUC. The area in common is delineated by a solid white line. The area observed with each pointing is indicated by the solid thin and dashed lines. Thus going from the lower left, we have field #1, which is shown with a thin green line, and clockwise around the square we have fields #2, #3 and #4.

3.4 DAOPHOT

A version of DAOPHOT (i.e., from the IDL version developed by W. Landsman[18]) will also be made available for the convenience of ESO ToolKit users. It has been automated and can be more effective than STARFINDER for the analysis of under-sampled images[16,17]. However, this has not yet been made into a facility programme and the widget interface has not been developed. However, a standard facility version is installed in the standard IRAF NOAO digiphot package that runs under any installation of IRAF.

3.5 Deconvolution and Spatially Dependant Regularisation of the PSF

Deconvolution is required for the accurate analysis of AO data on diffuse or nebular objects. Various existing algorithms are generally available to the user. For example, different implementations of the Lucy-Richardson algorithm are available for MIDAS, IRAF, STSDAS and IDL. Myopic deconvolution algorithms are also available (e.g. IDAC). However, for targets that have a significant extension or are not very close to the axis defined by the guide star (on average on average at the level of ten arcseconds in K-band in K-band), the PSF will change significantly (as seenn in Figure 3) and a Spatially Variant Deconvolution (SVD) is required. The simplest method is the patch approach to SVD, in which the complete image is considered as a family of small regions, where one tries to find a PSF star (and perhaps a photometric star) in each small patch. These calibration references, if available in each patch, would then be used for a Spatially Invariant Deconvolution (SID).

To our knowledge, there are no SVD packages currently available that properly handle the spatially variant PSF. In this discussion, we will consider a two-step approach, although a software package might very well combine them into a single programme. The first step is to homogenise or regularise the PSF so that it has the same form over the entire field of view. This requires first

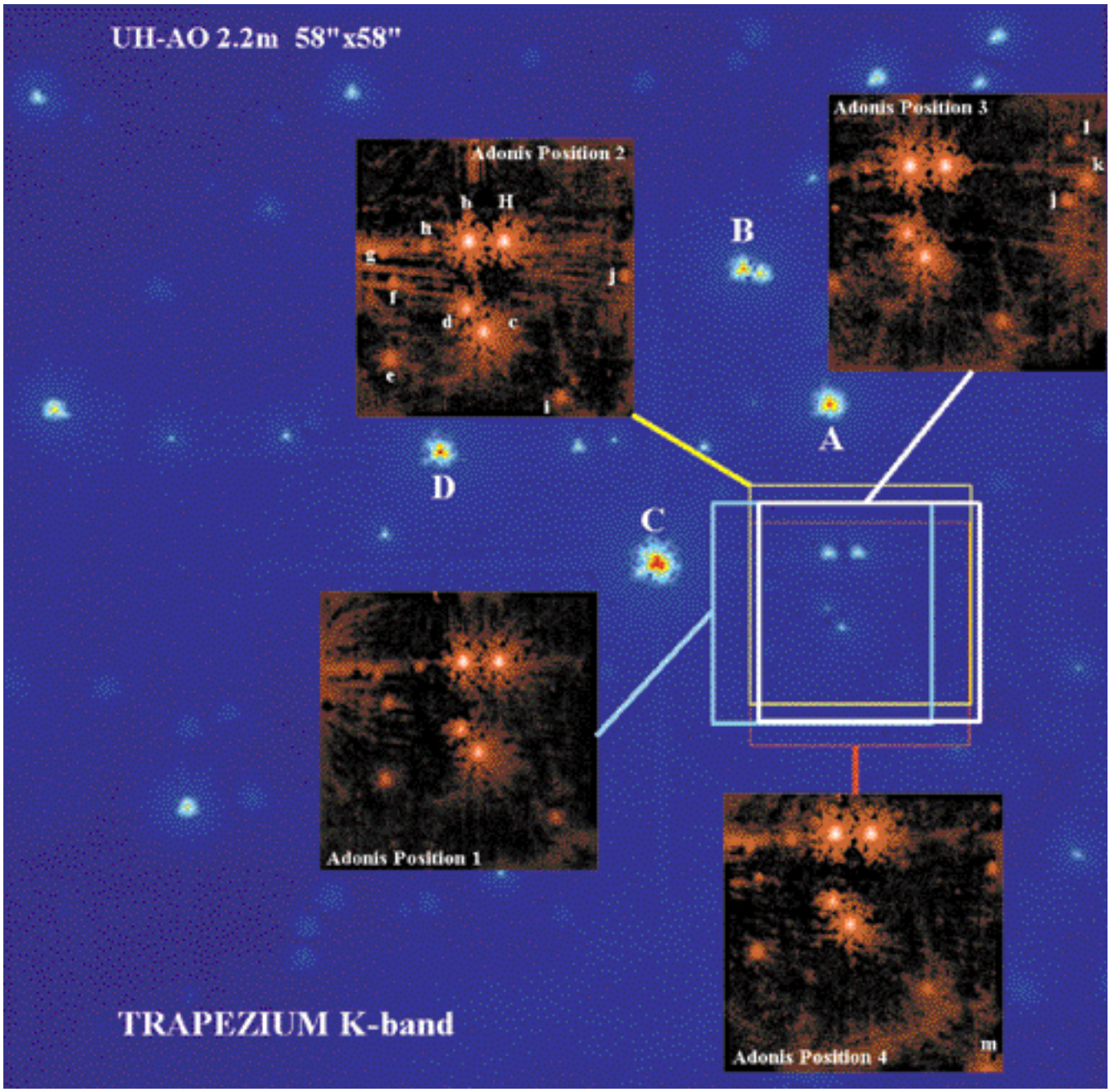

Figure 2: These images illustrate the High Strehl Stellar Observations conducted in the Trapezium in Orion. The large image (in blue) has been obtained in K-band on the 2.2 metre telescope[20] using the 13-elements UHAO[21] and the 1024 × 1024 QUIRC camera. Within this, we indicate the bright stars selected for guide stars for the observations. This entire cluster is named Θ[1] The square boxes indicate the position of the separate ADONIS FoVs obtained by Currie with 50 mas pixels to critically sample the core (2.5 pixels across the FWHM). The red im - ages are the bad pixel corrected, de-biased, flat fielded sky subtracted and averaged ADONIS SHARPII 256 x 256 images for each of the four pointings. Each box is 12.5 by 12.5 arcseconds.

calibrating the parameters that describe the an-isoplanatism. Then one would create the continuously variable PSF in a (currently not available) programme to make the PSF uniform. The second step is to apply one of the SIV algorithms to the homogeneous-PSF frame. Thus the key issue is the homogenisation algorithm. These issues are of paramount importance in the consideration of continuous distributions (nebular or galaxies) which might be at the edge of the isoplanatic patch so the evaluation of their photometric and astrometric properties are compromised by the PSF variation.

3.5.1 Spatially Dependent Homogenisation/Deconvolution

The development of a spatially dependent homogenisation/deconvolution has been a project of the University of Bologna and ESO. This programme would transform the image with a variable PSF, using a continuously parameterised model of the spatial variation of the PSF, into an image that has a uniform PSF. This procedure can be followed by a spatially invariant deconvolution of a conventional type (i.e., the Lucy-Richardson or PLUCYpackage, IDAC[9, 10], or other methods more adapted to the specific science objectives at hand).

3.5.2 Spatially Dependent Regularisation by Warping

This procedure corrects for the spatial variable PSF across the image, using a simple model of the variation of the PSF due to isoplanatic effects, i.e. the incorporation of the Gaussian elongation and broadening of the stellar images that has been demonstrated to be the dominant effect. This procedure has been demonstrated on AO data using an IDL implementation package[19]. These procedures have not been converted into a facility package at this time, nor have they have been widgetised.

3.6 Availability and Access to the ESO ToolKit

As these programmes are completed, they will be available to be downloaded from a Web page at ESO located at http://www.eso.org/science/papao/programs. IDAC is available at www.eso.org/aot, in the Adonis pages. The STARFINDER series will also be available on a mirrored Web Site at the University of Bologna. These programmes will also be offered as elements of the package for the standard distribution of IDL routines in the astron package[18]. For participation in the remote operation test in July-August 2000, contact dcurrie@eso.org.

4. Data Collection for the PAPAO

Without quantitative comparative evaluations, one cannot reliably select the proper software package for a particular science objective. Quantitative results from the comparison of the packages, using well-calibrated telescope data, are needed to select the proper software tool, and quantify the random and systematic errors of the science products. Thus, the data collection component of the PAPAO programme was designed to provide well-calibrated sets of data, that address the many parameters that were, and are, expected to significantly affect the procedures and accuracy of the AO data analysis. The uniformity of data collection procedures and the calibration procedures are extremely important to provide meaningful intercomparison of different observing conditions and different software packages. The primary body of data has been collected using the ADONIS system on ESO's 3.6-metre telescope at La Silla. In addition, we have received contributions of data from other observers using other AO systems. These external contributions are not calibrated in the manner discussed below. However, these external data frequently fill gaps, that is, data that cannot, or have not yet, been collected on ADONIS at La Silla.

4.1 ADONIS Data

In general, we have collected data sets with extensive calibration. Access to different data sets, with extensive calibration data is necessary to isolate, identify and quantify the different effects that have an impact on the photometric and astrometric accuracy. The identification of the optimal calibration data set and the attendant collection and analysis procedures is an evolving process. Some of the current procedures are discussed below. Here we describe the sources, standardised processing procedure, and output for specific data sets.

4.2 47 TUC Data Set from Adonis

In this discussion, we shall explicitly consider a few of the data sets obtained on the ADONIS System. The initial data set was collected in December 1998, consisting of images of the inner region of the globular cluster 47 TUC (NGC 104). These data, as well as all other data from ADONIS, were obtained by D. Currie.

4.2.1 The Central Crowded Region

This field, shown in Figure 1, for the evaluation of software performance, is near, but not exactly centred on the core of the cluster. The exact location was selected to overlap with observations that have been conducted using NICMOS with HST as well as observations by F. Ferraro. This field (as well as a series of overlapping fields) is shown in Figure 1. For the ADONIS system, we used the camera optics providing 100 mas pixels and a 25 arcsecond Field of View (FoV) with the Ks or K' filter. Thus, the PSF would have been badly under-sampled, if the Strehl ratio had been high (this data happened to have a relatively low Strehl ratio). These observations provide a set of unresolved objects of various intensities with relatively low background. The data consisted of four pointings obtained within an hour, where the pointing for each group was offset by a couple of arc-seconds. There are 10 images for each group, with an individual exposure time of 0.6 seconds. The bad pixels were removed, the images flat-fielded, the sky and dark frames subtracted, and then the ten successive images were combined using a median filter acting on each pixel. The images denoted T0 and T1 were then combined (with appropriate translation) to form T01. The same procedure was performed using the groups T2 and T3 to form T23. The PSF was independently obtained for each image (i.e. for T01 and T23) by the method defined by whatever Photometry Programme was being tested and the photometry was performed separately for each of T01 and T23. Analysis of this type was performed on this data set by several individuals at ESO and at Bologna. Some of these results are described below. This procedure was in general performed for each of the sets of results listed in the table. This 47 TUC data set was also distributed to the ten international groups in the AO data-processing community in November 1999, and is available to be downloaded at http://www.eso.org/science/papao/data/47tuc/.

4.2.2 The Outer, Less Crowded Region

At the same time that the above observations were recorded, observations were made of an adjoining region of the cluster, i.e. the region indicated by the black square in Figure 1. There were three purposes in observing this second field. The first purpose is to provide a less crowded region that will allow the application of the same algorithm to two regions with different degrees of crowding observed at the same time with the same atmospheric and AO system parameters. This test can evaluate the effects of crowding on different photometry and astrometry algorithms. This second less crowded region also allows a cleaner extraction of a (non-simultaneous) PSF, and gives a better estimation of the sky background.

4.3 ADONIS Data on the Trapezium

The two primary objectives of the Trapezium series was (1) to obtain well-calibrated data sets using ADONIS that have the high Strehl ratio that is representative of the expected Strehl ratios for CONICA/NAOS and (2) to obtain data sets to test the accuracy of software programmes that provide for the correction for the effects of an-isoplanatism.

4.3.1 High Strehl Data

We wish to obtain a well-calibrated and redundant data set that can be used for independent internal intercomparisons of the photometry and astrometry. The redundancy means that the data is recorded in a manner to provide a quantitative evaluation of the precision of the P&A. To achieve this with ADONIS observations we need a region with an acceptable number of stars for statistical security (ten or more stars in the FoV of the high-resolution camera mode, i.e., a region of 10 by 10 arc-seconds), and a very bright star, 6th magnitude or brighter, very near-by, to permit the optimal operation of ADONIS, and no star in the FoV that will saturate the detector. Such a region has been found in the Trapezium, and is indicated by the boxes in Figure 3. As shown in the figure, we point to four, highly overlapped regions. Thus in each of these four regions or patches, we can independently determine an internally defined PSF for that frame, and use that PSF to reduce the data in that frame. Thus we have four independent sets of the stellar magnitudes of the stars for which the stars obviously have the same magnitudes for all of the four pointings. The data were recorded with an exposure time such that the two stars H and b (~ 11th magnitude in K-band) are somewhat over-exposed in order to collect precise data on the wings or halos of the PSF. The stars c and d are well-exposed with the peak at 0.6 and 0.3 saturation. Finally, there is a cluster of ten fainter stars, the brightest of which is five magnitudes fainter than Ha.

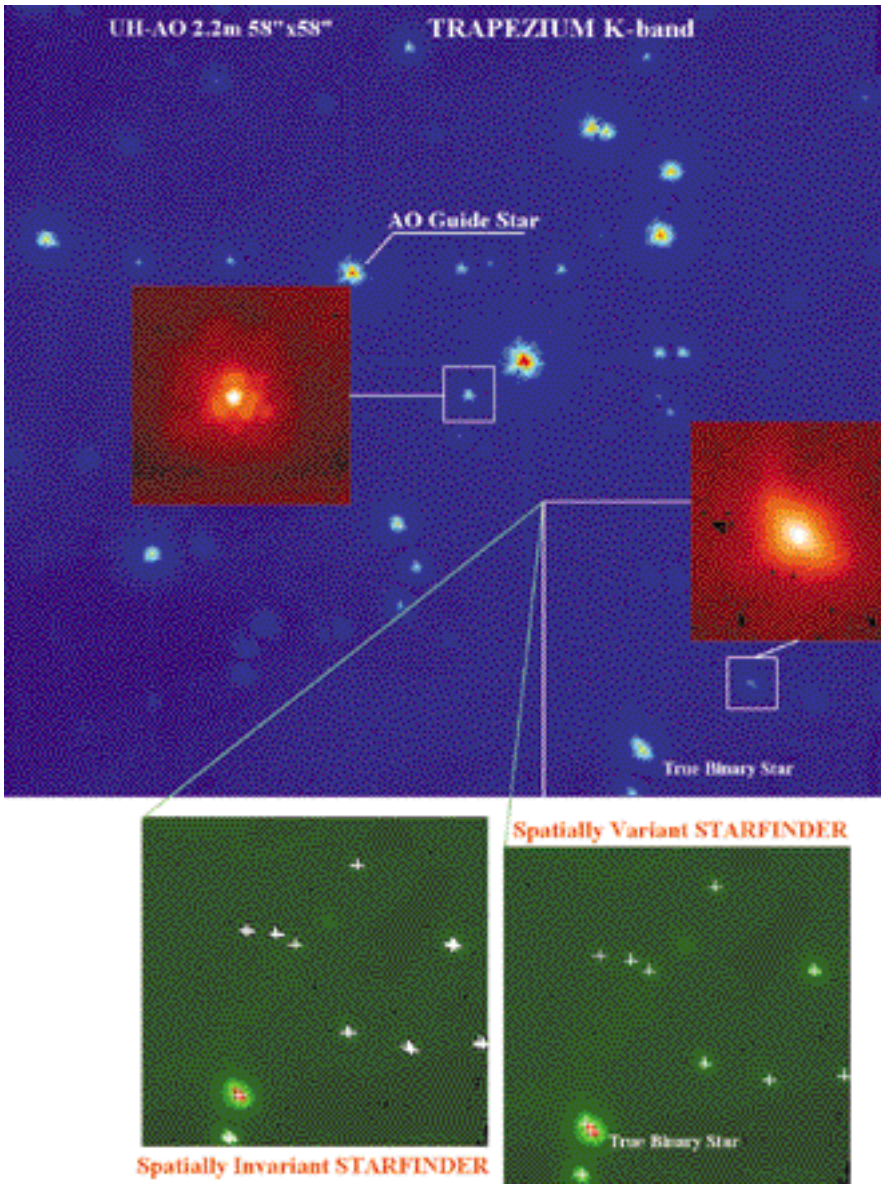

Figure 3: In the image of the Trapezium, we can see the effects of an-isoplanatism, that is, the change in the PSF in different parts of the image. At the bottom, we see the effects (on the left) of processing with a constant PSF(SI). We see in the left bottom panel that this soft - ware detected each of the distorted stars as a star with multiple components. On the right is the result of our continually parameterised model of the variable PSF that was used in the Spatially Variant Version of STARFINDER. Now all the distorted stars are identified as single stars (with the exception of the brightest star, which is actually the only true binary star in the field).

Finally, to permit the evaluation of the precision of the blind and myopic deconvolution algorithms, for each of the four pointings, a cube of short-exposure data was recorded. Thus the performance of myopic and/or blind deconvolution implementations can be tested. The photometric and astrometric precision can then be determined by inter-comparing the four independent myopic deconvolutions on the four independent cubes. The proximity of the bright stars allows the ADONIS data to be taken with a high Strehl ratio (32%). With the inter-comparison of the myopic deconvolution followed by the photometry and astrometry of the four patches in hand, one may then compare this precision with the precision obtained by the more conventional processing of the averaged cube of the same data. These data sets, bad-pixel corrected, flat-fielded, and sky subtracted, can be downloaded from http://www.eso.org/science/papao/data/trap

4.3.3 An-Isoplanatism Data Sets

A separate goal of PAPAO is to address the effects of an-isoplanatism, the variation of the PSF across the field of view as a function of the distance to the guide star. This effect is caused by the fact that the target star passes through a somewhat different sample of atmosphere than the atmosphere that is sensed and corrected by the AO systems which is locked on the guide star. An ideal data set could have been obtained in the manner of the UHAO image (background image in Figures 3 and 4). This entire region could be observed using different guide stars. This single 1024 × 1024 QUIRC image would then have contained the guide stars, and a large number of stars recorded simultaneously (with the same space variant PSF and the same an-isoplanatic parameters). However, the UHAO data was taken with certain science objectives, rather than the technical objectives of PAPAO. With the smaller 256 by 256 array of ADONIS, we must consider a different strategy. For this, we need to find an interesting field for which there are three or four bright stars at the edge of the isoplanatic patch, that is, within 25 arc-seconds of the centre of our Region of Interest (RoI). Preferably, these stars should be very bright, since the an-isoplanatic effects can be measured more easily with high Strehl images. While such fields are rare, the region discussed above (see Fig. 2) in the Trapezium satisfies all of these criteria. Thus we can collect data satisfying both the high Strehl ratio objectives and the an-isoplanatism objectives at the same time. This means that we can observe the same RoI (the RoI indicated in Figure 2) with up to four different guide stars. Since we have the four different pointings or patches for each guide star, we can determine the internal error structure, and thus cleanly isolate the effects of the an-isoplanatic errors and corrections. A proper programme to correct for the an-isoplanatic effects should result in good agreement for the data taken with A, C, and D used as guide stars. Most of the Trapezium data sets have been collected in the following manner. We observe the Region of Interest (RoI) using the first star (#1 C) as the Natural Guide Star. Four overlapping regions contained in the RoI (similar to the discussion of the observations of 47 TUC) are obtained. Then we start a similar procedure with the next Natural Guide Star, ((#1 D). We again observe four slightly overlapping images of the same RoI that was observed with ((#1 C as the guide star. Finally, we go to the third Natural Guide Star ((#1 A) and again collect four overlapping images.

4.4 ADONIS Data on η Carinae (the Homunculus)

We now address a quite different class of objects. In this case, we are interested in obtaining data sets to address the performance of deconvolution algorithms. These deconvolution algorithms are intended to improve the photometric SNR, and to remove artifacts for nebular or galactic objects, i.e., diffuse or continuous targets. In particular, this set of data should allow us to address the precision or accuracy of the recovery of the high-frequency components in the image.

4.4.1 Spatially Invariant Analysis

To this end, we are then interested in a quantitative evaluation of the accuracy and artifact introduction of spatially invariant deconvolution procedures. To address this, we need to select an object which extends over a major part of the ADONIS field of view, has a considerable amount of fine detail, an object for which we have other data that indicates the reality of the details of the structure, and finally, an object bright enough to allow a sequence of short exposures to test blind and myopic deconvolution algorithms and implementations. For this we have selected a portion of the Homunculus of η Carinae, perhaps the unique object which simultaneously satisfies all these criteria. We have previously produced astrometrically rectified images for the studies of the motion of the clumps in the homunculus[13, 22, 23]. There is a range of brightness, and very short exposures are adequate to obtain a good signal-to-noise ratio, even with a 50 milli-arc-second resolution. η Carinae itself is bright enough to be an excellent guide star, sufficient to get good Strehl ratios for the Homunculus images. This data has been bad-pixel corrected, flat-fielded, and sky and dark subtracted. The resultant images for two overlapping regions observed in K-band with 50 mas/pixel are shown in Figure 4, where they can be compared to our image from the WFPC in Hα. These images have been analysed at ESO, in particular, applying the Lucy-Richardson algorithm and myopic deconvolution in the implementation of IDAC. The results of these deconvolutions have been analysed on a pixel-by-pixel evaluation to address the performance of the algorithms, using various figures of merit. In the future, we plan to address this behaviour in terms of the spatial frequency, that is, averages over small blocks of pixels in order to separate the high frequency performance from the lower frequency performance.

4.4.2 Data for An-Isoplanatic Effects in Continuous Targets

However, even with the new NGS AO systems that are being developed and installed on the 8-metre-class telescopes, the lack of guide stars in the very immediate vicinity of the target will results in strong an-isoplanatic distortion of the targets shape and brightness distribution, as indicated in Figure 3. For this reason, we wish to explore the post-detection software methods that correct for the influence of a PSF that changes its shape over the field of view. In particular, we wish to determine the effectiveness of the very few spatially variant deconvolution algorithms to remove the effects of the an-isoplanatic variation of the PSF across the observed field of view. Since we do not have the God's Truth, we need to again develop a procedure of observing with multiple Natural Guide Stars and look for internal consistency. In this type of analysis, we will determine the photometric structure of the object, as determined independently from each of the data sets. The P&A from a properly operating software deconvolution programme, or more precisely the spatial frequency components of the P&A should agree, even though they have used guide stars that are at different distances and different orientations with respect to the RoI. However, to perform these observations in a reasonable amount of telescope time, we need a very bright nebular object that has, within tens of arcseconds, at least three stars bright enough to be natural guide stars for ADONIS. In the selection of a portion of the homunculus of η Carinae, we have three guide stars within 15 arcseconds, and a total of five guide stars within 25 arcseconds of the centre of the region of interest as shown in Figure 5. All five of these stars are brighter than 11th magnitude, quite acceptable as guide stars for ADONIS. Thus we have a rather ideal configuration to test the continuous distribution.

The relatively bright guide stars are at distances of 6 arcsecond (mv = 6), 8″ at 10th, 8″ at 10th, 12″ at 12th and 25″ at 11th. This makes it a unique object for the performance of these tests. In addition, we have an extensive set of WFPC data for comparison of the small linear features. To allow the precise comparison, we took two views of the RoI, slightly translated. In addition, we observed the four stars at a greater distance from the RoI to obtain the parameters that describe the degree of anisoplanatism.

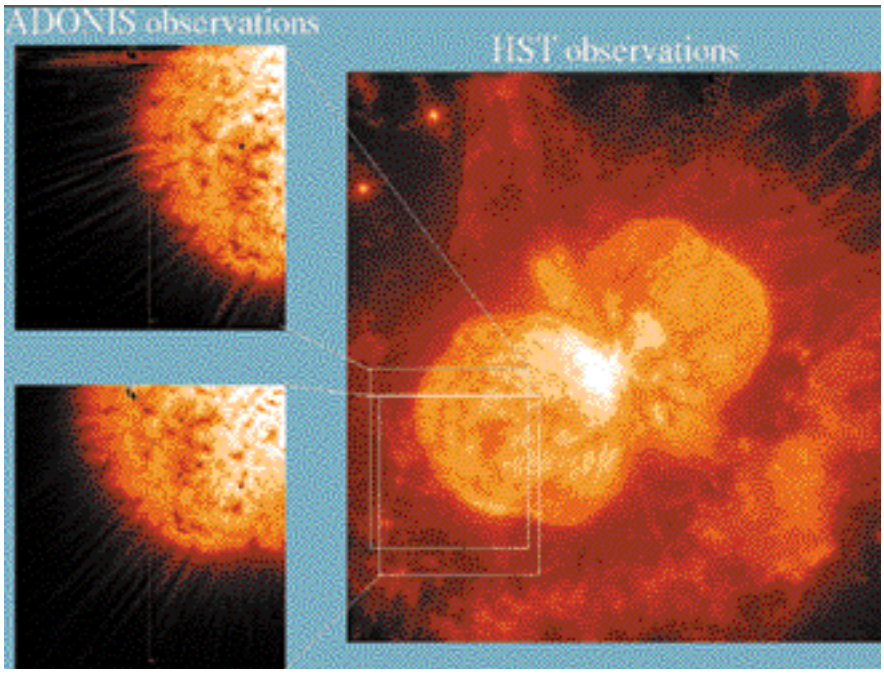

Figure 4 illustrates the data set that has been used for the analysis of nebular objects. The large figure on the right from the Hubble Space Telescope shows the regions selected for the ADONIS observations (the central part of the SE lobe of the homuculus of η Carinae). This was selected because it is bright at K-band, allowing short exposures even at 50 mas resolution, has a number of relatively bright guide stars near it i.e. at distances of 6 arc second (mv=6), 8" at 10th, 8" at 10th, 12" at 12th) and 25" at 11th.

4.5 Summary of Data Sets for Community Analysis

Table 1 describes some of the data sets that have been obtained using ADONIS and other systems, and are being prepared for use, internally and externally over the next year. Well-calibrated data, obtained under a variety of conditions with the same calibration procedures, are necessary to separate the various parameters that affect the accuracy of the data analysis by various software programmes. They are in various states of pre-processing, calibration and validation. All are in K-band unless otherwise stated. There are various criteria that describe the parameters that will affect the collection and analysis of AO data. We give rough indications of the domain in which each of the data sets falls. The average density of stars per arcsecond roughly indicates the number of stars that may be expected to be found in the wings of adjacent stars. This of course depends upon the seeing at the time, but this column gives an estimate of the density in the most critical region for the AO correction. An indication of the Strehl ratio is given. A precise definition is difficult in these crowded fields, and the use of the Strehl ratio of a calibration star must be checked for the stability. Data sets that are currently available are indicated by a "+" and are indexed at http://www.eso.org/science/papao/data/47tuc/

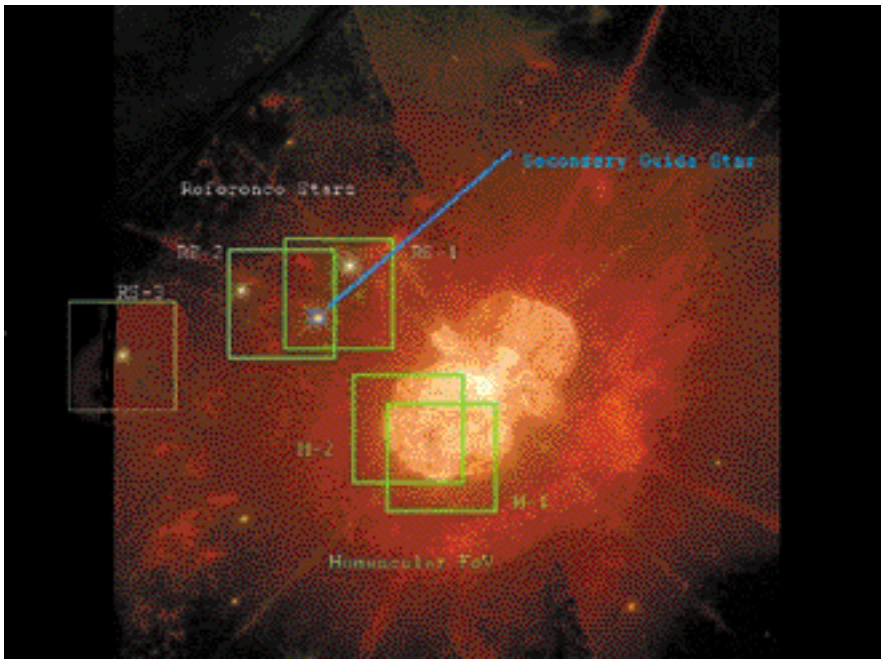

Figure 5: This uses our HST image to illustrate the ADONIS data sets obtained by Currie to address the deconvolution procedures with an-isoplanatic effects for nebular objects. The first two regions (H-1 and H-2) were selected for analysis (these are the regions shown in Figure 4). They are the central part of the SE lobe of the Homunculus. The other three regions (RS-1, RS-2, and RS-3) were selected to evaluate the an-isoplanatic parameters when the central star was being used for the guide star. We later looked at the same five patches but using first one then another of the outer stars as the natural guide star. For scale, each of the green boxes is 12.5 arcseconds on a side. We have an extensive set of WFPC data for compari - son of the small linear features.

The fourth column indicates the sampling, the first number being the number of pixels in the theoretical diffraction-limited core. This addresses issues in obtaining and translating the core of the PSF. The fifth column is the (linear) number of pixels in the wings caused by the atmospheric effects. This indicates the area in which the photometry is strongly affected by the variability of the lower levels of the PSF. The remaining data sets will be placed upon the PA-PAO Web Site as the pre-processing and calibration isare completed.

5. Algorithm Testing Component of the PAPAO

The portion of the PAPAO programme concerning the testing of the various photometry and astrometry algorithms divides into two parts. The first part is to develop numerical simulated data to evaluate performance of each of the packages of software programmes. The results of this analysis will be provided on the web page. This will illustrate the science performance of the software programmes in the ESO ToolKit, results at the level that might be obtained by a general observer, that is, an individual who is not an expert in AO. Some of the initial results of this analysis will be presented below, as an example of the type of analysis that will be developed. A second part of the algorithm testing programme involves the distribution of selected field-data sets to be processed by those individuals who have developed the code for various photometry and astrometry software packages that are of interest for AO data. The main objective of this second partcomponent is to identify and select the best programmes and/or algorithms to develop, test, and implement the next generation of the ESO ToolKit. The second objective in this second portion of the algorithm testing part is to discover better procedures for the use of the publicly available software.

Table 1.

Target/ DataSet	Star Density	Strehl Ratio	Samples/ # pixels FWHM in wings		Description and Comments
47 TUC_A +	0.8	low	1.5	6	This data set is composed of 25″ by 26″ images described in the previous section, and it was distributed to ten groups for external testing by experts in November 1999
47 TUC_A_2 +	0.8	low	1.5	6	This data set was obtained at approximately the same time as 47 TUC_A, but it has a lower stellar density. It will thus be used to compare the relation between the crowding and the photometric and astrometric precision when the atmospheric conditions and AO system parameters are similar.
T Cluster 25.0	high	high	3.0	6	This is an ADONIS data set augmented with synthetic stars each of which has the proper noise and PSF (both in shape and in an-isoplanatic variation obtained for actual observation). This serves as a set of absolute calibrators at high crowding.
47 TUC_B +	0.8	med	1.5	6	This data set contains 100 frame sets especially obtained for testing blind and myopic deconvolution programmes
47 TUC_B_2 +	0.8	med	1.5	6	This data set contains 100 frame sets, especially obtained for testing various blind and myopic deconvolution programmes. It has a lower density of stars than 47 TUC B.
Homunculus +	—	med	3.0	12	These are 100 frame sets to test various implementations of blind and myopic deconvolution on a continuous (or nebular) object that has both a large dynamic range and many very fine features.
Trapezium +	low	32%	3.0	12	This data set addressed the an-isoplanatic effects for unresolved objects with relatively high Strehl ratios. The low stellar density allows the isolation of the crowding versus an-isoplanatism (although having fewer stars causes some statistical problems).
Homunculus +	—	high	3.0	12	This is an H-band data set for an extended target. Multiple exposures are taken to investigate and quantify the an-isoplanatic effects (see paragraph on an-isoplanatic data sets for homuncular images)

Table 2.

Programme	Analyst	# Stars Analysed	Dynamic Range	RMS Magnitude 14 stars 3.9 mag Stdev	error	65 stars 4.4 mag Stdev	error
SF-9905	Tordo	120	7.14	0.055	0.010	0.033	0.003
SF-9905	Tordo	127	7.14	0.059	0.011		
SF-9905	Tordo	175	7.37	0.087	0.016		
DAOPHOT	Tordo	73	4.75	0.056	0.011	0.040	0.004
SF-9905	Naesgarde	23	2.1	0.0253	0.005		
DAOPHOT	Naesgarde	23	2.1	0.0144	0.003		
SF-9909	Diolaiti	266	9.0	0.040	0.008	0.023	0.002

** This analysis excludes three out-liers, since the edge of the field was not excluded from the comparison calculation.
• Two versions of STARFINDER have been used. SF-9905 was installed by E. Diolaiti on the ESO computer system in May 1999 and has been available for evaluation in Garching. SF-9909 was a later version used by E. Diolaiti for some of his tests conducted at Bologna Observatory.

5.1 Results of the Algorithm Testing Component of the PAPAO

In Table 2 we list the comparative results obtained by using the various different software programmes. In each case, we compare the magnitudes (and positions) obtained for each different pointing or patch. Then the magnitudes or positions of a given star obtained in each of the patches are compared. The mean magnitude or position over the entire frame is zeroed, and the residuals are plotted as a function of magnitude. The dependence of the size of the errors on the stellar magnitude gives an indication as to the source of the error: photon noise, read noise, PSF noise or flat-fielding errors. Clearly we are not addressing all the possible errors, but the starting point is here. Then we can consider the effect of significantly different atmospheric conditions, different optimisations of the AO system, as well as methods of correcting the saturation and extraction of the PSF.

We first consider a set of 20 bright (and some fainter) stars, then a set of the brightest 60 stars, and then a set of the brightest 120 stars. Stars at the edge of the field and other anomalies have been eliminated from the numbers for all of the groups (thus each run uses the same set of stars). The RMS Magnitude indicates the differences between the measured magnitude of a star in T01 and the measured magnitude of a star in T23. The average value of all the stars over the field is set to zero, so we are evaluating the differences a given software programme measures for the same stars, and not including the zero point issue. In general, we see that the range of the internal errors in the measurements is between 0.088 and 0.014 magnitudes, that is, between 8.4 and 1.3 per cent.

The set of 14 stars analysed in the right panel of Table 2 was selected in order to have a common set among all analysts (who had analysed this data set within different research objectives). For the case of 14 stars the purely statistical error bars are about the values of the standard deviation found in the table. Therefore, the difference between the P&A programmes which were tested is not statistically significant (two sigma) for this small set of stars. However, it is clear that the performance is about a factor of thirty worse than the theoretical performance, that is, the photometric noise is much worse than the noise to be computed from the photon statistics, the sky noise, and the readout noise. On the other hand, this may be contributed by the problems of flat fielding that have not been explicitly quantified on this data. For the case of 65 stars, the purely statistical error bars are listed. The differences are marginally significant. Note that earlier tests of the ROMAFOT programme (several analyses based upon a data set obtained on NGC 1850) indicates that it obtained precision at about the same level. Similar results, with precision at the level of between 5 and 20 mas, have been obtained for the astrometric measurements of the same image of 47 TUC. These statistical aspects indicate another area where a careful integrated plan of data collection and data analysis is essential for obtaining statistically significant comparisons.

Note that the errors found in these ESO analyses are smaller (better accuracy) than those found in the literature. On the other hand, we have not included the absolute errors in the photometry. However, the errors found are still more then ten times the magnitude of the expected errors computed from the photon noise (which is dominant in this domain), readout noise and sky noise.

5.2 Flat-Fielding Effects in AO

Another source of errors for precise photometry is errors of various types in the flat-fielding procedure. In principle, we may expect the accuracy of the flat-fielding to be of the order of 0.3 to 1%. This is the experience of SOFI, where these procedures have been checked in detail. However, these results would be the end product of an extensive investigation that has not yet been carried out on the ADONIS SHARPII camera. One must address the problems of reproducibility as well as the difference between a flat field produced by a continuous distribution (the sky) and that produced by points of light, i.e. the shading or illumination corrections. These have not yet been checked independently, so there is an unknown component in the photometric results presented here that is due to the flat fielding problems. A study of such flat-fielding effect is important for high-accuracy AO photometry. It will also require the collection of test data from the telescope addressing higher dynamics range. Such observations are difficult on the SHARP II camera, since operating with the brightest object in saturation is not acceptable for this array. Thus the noise must be reduced by repeated observations, so improvements go at the square-root of the time, requiring significant telescope time.

5.3 Effectiveness of Prior Deconvolution

Traditionally, it has been presumed that one could improve the photometry and astrometry that could be obtained from AO data by performing a deconvolution on the image before measuring the intensities and position of the stars. In this section, we address the results of performing a Lucy-Richardson or a myopic deconvolution before performing the photometry. In this case, we have used our 47 TUC image, and performed the photometry. Then the image was deconvolved, using the Lucy-Richardson algorithm and IDAC programme. For each of the deconvo-

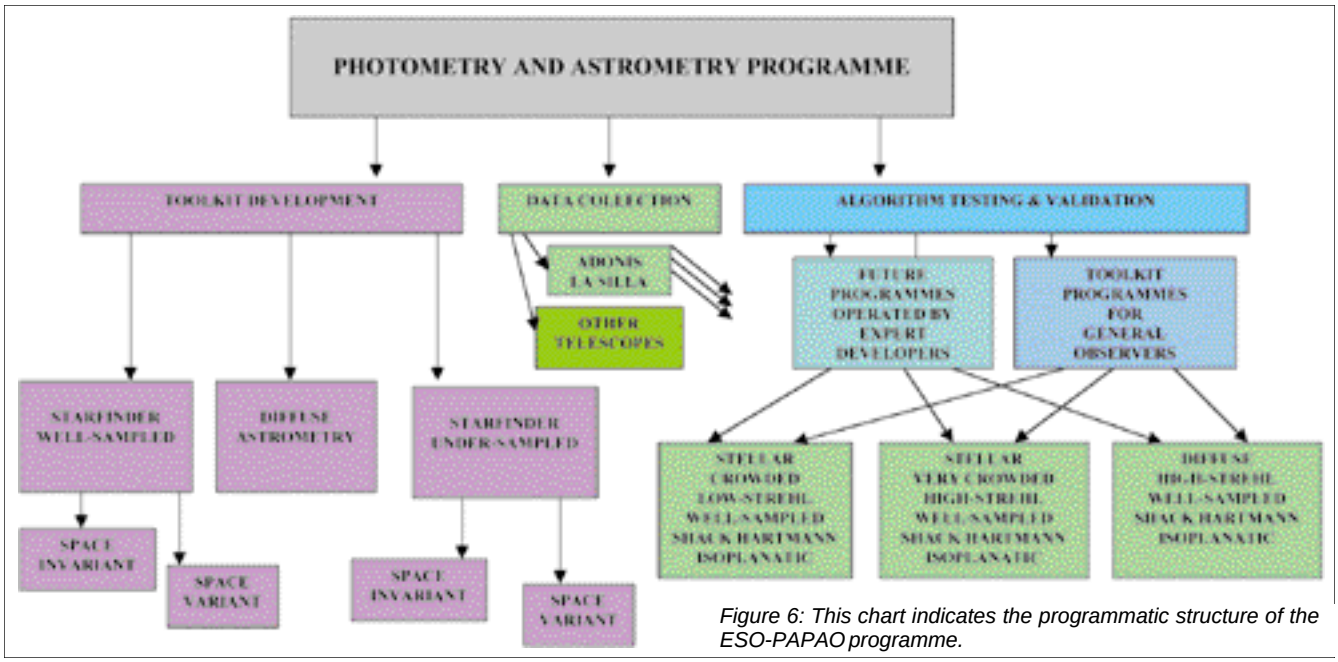

Figure 6: This chart indicates the programmatic structure of the ESO-PAPAO programme.

lution algorithms, tests were performed with both 500 and 2500 cycles. This was followed by the use of DAOPHOT and/or STARFINDER for the photometry.

The last column in Table 3 directly compares the photometric precision when using deconvolution referenced to the photometric precision obtained on the image with no deconvolution. Thus we see that the use of deconvolution degrades the photometric accuracy. More precisely, this expresses the differences between the magnitudes determined for the two patches (T01 and T23) when using STARFINDER before and after deconvolution. Thus it indicates the precision obtained with a given photometry software programme applied to the patches with different pointings before and after various deconvolution procedures. For example, after 2,500 iterations of IDAC, the photometric errors in the RMS Magnitude sense were larger by a factor of three than if the photometry had been performed with no deconvolution. These deconvolutions were done with the standard rules or default procedures for the use of the deconvolution algorithms. It may be that these results could be improved by the expert use of the deconvolution algorithms. If this is the case, we would hope to be able to incorporate these improvements into the procedures that would be distributed in the ToolKit. Thus, if there is better performance available with expert intervention we wish to define the operating rules that allow a non-expert to achieve the same results. However, these results by K. Naesgarde and J. Liwing using IDAC 2.4 on a stellar cluster agree almost completely with an analysis of a binary system performed by J. Christou and D. Bonaccini[24].

5.4 Role of Under-Sampled Images

The issue of the degree of sampling has been critically important on the ADONIS system, and will remain important on the 8–10-metre telescopes. In principle, we should always critically sample the data, that is, have more than two pixels in the diffraction-limited core of the image. Practically, this is normally feasible (depending upon the relation between read noise and target brightness) for single objects, but for targets like stellar clusters, we need a statistically significant sample of stars. This is a force toward less than critical sampling (presuming the AO camera system allows the astronomer the choice of different spatial sampling rates). As we go to the visible, it will also be important in terms of read noise. However, there is no information available at present as to the dependence of the feasible photometric accuracy as a function of sampling rate to guide the astronomer. Initial studies have been conducted under the PAPAO programme. Similar analysis of under-sampled images showed a reversed effect, the DAOPHOT performed about a factor of two better than STARFINDER. In order to obtain a set of under-sampled images with all of the required properties for the astrometric studies in a reasonable time scale, we have used data obtained from our observations with WFPC and WFPC2 of the HST[25,22,23]. The results indicated that DAOPHOT did significantly better than the STARFINDER (to be expected on the basis of the algorithm structure of STARFINDER). This appears to be due to the procedure in DAOPHOT for determining the PSF. It starts with an analytically defined initial guess and looks for corrections from the data. This has the advantage that the analytic core can be translated more precisely than the estimate obtained directly from the data as in STARFINDER. However, on the version of DAOPHOT we have used (in the astron library of IDL), we must use a double Gaussian version, and cannot insert and fit the best analytic model that we expect from the physics of the AO process.

Table 3.

Deconvolution Method	# Iterations	Standard Deviation	Relative Photometric Accuracy
None		0.0144	1.00
Lucy-Richardson	500	0.0157	0.83
Lucy-Richardson	2,500	0.0485	0.33
IDAC	500	0.0661	0.25
IDAC	2,500	0.0463	0.31

6. Current Status of PAPAO Programme

6.1 Preliminary Conclusions

6.1.1 Numerical Results on Stellar Clusters (i.e. Unresolved Targets)

We have three primary conclusions at this time. These are based upon analysis at ESO, that is, the analysis in the spirit of the General ESO observer, rather than by the developers of the codes. We still await the expert analysis results.

(1) For Well-Sampled Images with relatively low Strehl ratios, and relatively low levels of nebulosity, the three photometry and astrometry programmes that we have tested, i.e. STARFINDER, DAOPHOT and ROMAFOT give similar accuracy. While there are statistically significant differences, in general, they are relatively fine points.

(2) When more similar PSF characterise the data, in a manner that also reduced the flat-fielding errors, the photometric and astrometric errors are reduced. STARFINDER does significantly better, when the deleterious effects of PSF variation and flat-fielding are reduced.

(3) For Under-Sampled HSTImages, DAOPHOTperforms significantly better than STARFINDER. This may be due to the DAOPHOT assumption of a functional representation for the PSF that is reasonably correct, and which can be analytically translated to the centre of another star. This helps both in the formation of an averaged PSF and for the star that is being measured.

(4) For stellar photometry, the prior use of deconvolution (at least in the forms of Lucy-Richardson and myopic deconvolution) does not improve the precision of the photometry. Of course the primary use of such algorithms is for morphology and astrometry. Preliminary results on the photometry of continuous distributions are inconclusive.

Finally, a large improvement is required in order that the AO photometry and astrometry may reach the desired levels of accuracy, although a large part of this may be due to the flat fielding that also affects non-AO infrared photometry.

6.1.2 Current Programmatic Issues

The initial domains of performance have been identified for several software packages. We have seen that the procedures for the determination of the PSF must be investigated more completely. The widget-based Spatially Invariant STARFINDER will be available in July of 2000. The first set of data (well-resolved low Strehl stellar clusters) have been distributed to the community. A second set (well-resolved, high Strehl stellar clusters with calibrators) is available on the PAPAO Web Site at http://www.eso.org/science/papao/

6.2 Invitation to ESO Community

We invite and strongly encourage all interested to participate in the PAPAO programme. This participation may take a number of different forms. This may consist of applying your favourite photometry and/or astrometry algorithm to some of the calibrated PAPAO data sets. It may also consist of contributing your algorithms for testing by the broader community, or the contribution of your data sets to be used in PAPAO.

FREE TEST OF STARFINDER for ESO COMMUNITY

ESO is supporting a test of STARFINDER and the RSI software package ION. This test will occur from mid-June through mid-August. This will permit remote users to test STARFINDER on some of the data sets discussed in the article. We would be very interested in reports of the results, both concerning the software, and concerning the numerical results. Please contact the author at dcurrie@eso.org for the appropriate procedures to cross the ESO firewall.

Data sets with a single frame FoV that are significantly larger than the isoplanatic patch, and that are recorded for two or more guide stars that are separated by approximately 10 arc seconds, would be particularly valuable. Finally, we are interested in working with beta testers of the programmes to be released within the ESO ToolKit. In July and August, we will be testing the software package ION that allows remote participants to use STARFINDER on the ESO computers and IDLlicense. If you are interested in participating in these tests, please contact dcurrie@eso.org

7. Acknowledgements

We would like to acknowledge the generous allocation of ESO telescope time to the AO data reduction programme PAPAO, and the support of the members of the 3.6-metre team at La Silla. We would also like to acknowledge the contribution of data, for our engineering purposes, by L. Close[20], F. Rigaut, and S. Hippler.

References

[1]Currie, D.E., Diolaiti, D., Bonaccini, S., Tordo, K., Naesgarde, J., Liwing, O., Bendinelli, G., Parmeggiani, L. The ESO Photometric and Astrometric Analysis Program for AO: A Programmatic and Numerical Analysis Proc. of SPIE Vol. 4007 Adaptive Optical Systems Technology Editor: P. Wizinowich, #4007–72 1–12 (in press) (2000).

[2]Currie, D.G., E. Diolaiti; S. Tordo; K. Naesgarde, J. Liwing, O. Bendinelli; G. Parmeggiani, L. Close, D. Bonaccini. (1999) ESO Photometric and Astrometric Analysis Program for Adaptive Optics ADASS-IX 1999.

[3]Diolaiti, D., Bendinelli O., Bonaccini D., Parmeggiani G., & Rigaut F. STARFINDER: an IDL GUI based code to Analyze Crowded Fields with Isoplanatic Correcting PSF Fitting (1998) in ESO/OSA - Topical Meeting on Astronomy with Adaptive Optics., ed. D. Bonaccini (Garching b. Meunchen, ESO), p.175).

[4]Diolaiti, E. et. al. Proc. of SPIE Vol. 4007 Adaptive Optical Systems Technology Editor: P. Wizinowich, #4007–74 1–12 (in press) (2000).

[5]Diolaiti, E., D. Currie, O. Bendinelli, G. Parmeggiani, L. Close, D. Bonaccini (1999) Astronomical Data Analysis Software and Systems – IX 1999.

[6]Bonaccini, D., Prieto, E., Corporon, P., Christou, J., Le Mignan, D., Prado, P., Gredel, R., and Hubin, N., (1997) "Performance of the ESO AO system ADONIS, at La Silla 3.6m telescope, SPIE Proceedings Vol 3126, "Adaptive Optics and Applications", Tyson and Fugate Eds.

[7]http://www.ls.eso.org/lasilla/Telescopes/360cat/adonis/

[8]http://www.eso.org/projects/aot/aowg

[9]Christou, J.C., Bonaccini, D. et. al (1999) "Myopic Deconvolution of Adaptive Optics Images" *The Messenger*, No. 97, p. 14–22, http://www.eso.org/gen-fac/pubs/messenger/

[10]Christou, J.C., Ellerbroek, B., Fugate, B.Q., Bonaccini, D. and Stanga, R. (1995), Rayleigh Beacon Adaptive Optics Imaging of ADS 9781: Measurements of the Isoplanatic Field of View, *ApJ*, 450, 869–879.

[11]Close, L. M. (2000) SPIE 4007 "A Review of Published Galactic and Solar System Science: A Bright Future for Adaptive Optics Science".

[12]http://www.eso.org/instruments/naos/index.html

[13]Currie, D.G. and D.M. Dowling. (1999) "Astrometric Motion and Doppler Velocity" Eta Carinae at the Millennium, ASP Conference Series, Vol. 179 J.A. Morse, R.M. Humphries, and A. Damineli, eds.

[14]Dowling, D.M. (1996) "The Astrometric Expansion and 3-D Structure of eta Carinae" University of Maryland, Ph. D. Thesis.

[15]Currie, D.G., Dowling, D.M., Shaya, E.J., Hester, J., Scowen, P., Groth, E.J.; Lynds, R., O'Neil, E.J., Jr.; Wide Field/Planetary Camera Instrument Definition Team "Astrometric Analysis of the Homunculus of eta Carinae With the Hubble Space Telescope" 1996, AJ, 112, 1115.

[16]Naesgarde, K. (1999) "Accuracy in Differential Photometry – STARFINDER vs. DAOPHOT" Master's Thesis TRITA-FYS #XXX, Stockholm.

[17]Liwing, (1999) "Accuracy of Different Methods for Differential Astrometry" Master's Thesis TRITA-FYS #XXX, Stockholm.

[18]Landsman, W.B. (1995) "The IDL Astronomy User's Library" Astronomical Data Analysis Software and Systems IV, ASP Conference Series, Vol. 77, 1995, R.A. Shaw, H.E. Payne, and J.J.E. Hayes, eds., p. 437.

[19]Avizonis, P. V.(1997) Ph. D. Thesis University of Maryland.

[20]Simon, M., Close, L.M., Beck, T.L. "Adaptive Optics Imaging of the Orion Trapezium Cluster" (1999) *AJ*, **117** 1375–1386.

[21]Roddier, F., Northcott, M., Graves, J.E., "A simple low-order adaptive optics system for near-infrared applications" 1991 *PASP* **103** 131–149.

[22]Currie, D.G., D.M. Dowling, E. Shaya, J.J. Hester, HSTWFPC IDTand HSTWFPC2 IDT "3-D Structure of the Bipolar Dust Shell of eta Carinae" (1996) "Role of Dust in the Formation of Stars, Garching bei Muenchen, Federal Republic of Germany, 11–14 September 1995, Proceedings of

the ESO Workshop, Käufl, H.U. and Siebenmorgen, R. (Ed.) Springer-Verlag, 89–94.
[23]Currie, D., D. Le Mignant, B. Svensson, E. Diolaiti, S. Tordo, K. Naesgarde, J. Liwing, O. Bendinelli, G. Parmeggiani, D. Bonaccini "Hyper-Velocity Jets and Homuncular Motion in eta Carinae: an Application of the Fabry-Perot, ADONIS and AO Software" SPIE Vol. 4007 AO Systems Technology Editor: P. Wizinowich, # 4007–75, 1–12 (in press) (2000a)+
[24]Christou, J. and Bonaccini, D. "An Analysis of ADONIS Data, tau Canis majoris – Deconvolution".
http://www.ls.eso.org/lasilla/Telescopes/360cat/adonis/html/datared.html#idac
[25]Hester, J.J.; Light, R.M., Westphal, J.A., Currie, D.G., Groth, E.J.; Holtzmann, J.A., Lauer, T.R., O'Neil, E.J., Jr. "Hubble Space Telescope imaging of Eta Carinae" 1991 *AJ* **102**, 654–657.

STARFINDER: a Code to Analyse Isoplanatic High-Resolution Stellar Fields

E. DIOLAITI[1], O. BENDINELLI[1], D. BONACCINI[2], L. CLOSE[2], D. CURRIE[2], G. PARMEGGIANI[3]

[1]Università di Bologna – Dipartimento di Astronomia; [2]ESO; [3]Osservatorio Astronomico di Bologna

1. Introduction

StarFinder is a code designed to analyse Adaptive Optics images of very crowded fields. A typical AO observation has a well-sampled and complex-shape PSF, showing a sharp peak, one or more fragmented diffraction rings and an extended irregular halo. The approach followed in StarFinder (Diolaiti et al., 1999a, 1999b, 2000) is to analyse the stellar field with a digital image of the PSF, without any analytic approximation.

Under the assumptions of isoplanatism and well-sampling, StarFinder models the observed stellar field as a superposition of shifted scaled replicas of the PSF lying on a smooth background due to faint undetected stars, possible faint diffuse objects and noise.

The procedure derives first a PSF digital template from the brightest isolated field stars; then a catalogue of presumed objects is formed, searching for the relative intensity maxima in the CCD frame.

In the following step the images of the suspected stars are analysed in order of decreasing luminosity; each suspected object is accepted on the basis of its correlation coefficient with the PSF template; the relative astrometry and photometry of the source are determined by means of a fit, taking into account the contribution of the local non-uniform background and of the already detected stars.

At the end of the analysis it is possible to remove the contribution of all the stars detected up to this point and perform a new search for previously lost objects (e.g. secondary components of close binaries).

StarFinder is not a general-purpose algorithm for object recognition: it should be intended as a tool to obtain high-precision astrometry and photometry in adequately sampled high-resolution images of crowded stellar fields. In practice it can be applied not only to high-Strehl AO observations, but also to low-Strehl images. The code versatility has been also proved by an application to a set of HST NICMOS images (Section 3.3); in Aloisi et al. (2000) there is a comparison between our results and those obtained by DAOPHOT.

Much more intriguing and difficult to solve is the case of a field with space variant PSF, due to anisoplanatic effects in AO observations. In general the analysis of an anisoplanatic field requires the knowledge of the local PSF. The extension of StarFinder to the space variant case is in progress. Preliminary results have been presented at the ESO/SPIE meeting Astronomical Telescopes and Instrumentation 2000 (Diolaiti et al., 2000).

2. Analysis Procedure

2.1 PSF determination

The PSF is treated as a template for all the stars in the isoplanatic patch, so its knowledge is of basic importance for a reliable analysis.

The PSF extraction procedure included in StarFinder is based on the median average of a set of suitable stars selected by the user. Before being combined they are cleaned from the most contaminating sources, background-subtracted, centred with sub-pixel accuracy and normalised. The centring is performed by an iterative shift of the stellar image in order to cancel the sub-pixel offset of its centroid. The halo of the retrieved PSF is then smoothed, applying a variable box-size median filtering technique.

The PSF extraction procedure is able to reconstruct approximately the core of

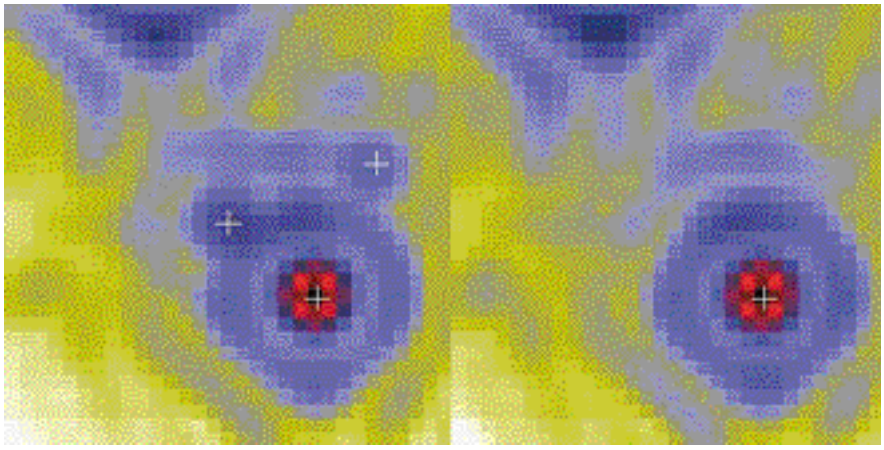

Figure 1: Left: sub-image extracted from a (simulated) stellar field, including the central star to be analysed, a brighter source which is already known, a fainter one, which will be examined later, and the PSF feature of a much brighter star, represented by the structure in the upper-left part of the sub-image. Right: corresponding sub-region extracted from the stellar field model, containing one replica of the PSF for each star detected so far.